Stem Cell Reports, Volume *16*

Supplemental Information

CALR frameshift mutations in MPN patient-derived iPSCs accelerate maturation of megakaryocytes

Kathrin Olschok, Lijuan Han, Marcelo A.S. de Toledo, Janik Böhnke, Martin Graßhoff, Ivan G. Costa, Alexandre Theocharides, Angela Maurer, Herdit M. Schüler, Eva Miriam Buhl, Kristina Pannen, Julian Baumeister, Milena Kalmer, Siddharth Gupta, Peter Boor, Deniz Gezer, Tim H. Brümmendorf, Martin Zenke, Nicolas Chatain, and Steffen Koschmieder

Supplemental Information

CALR frameshift mutations in MPN patient-derived iPSCs accelerate maturation of megakaryocytes

Kathrin Olschok[1,2,*], Lijuan Han[1,2,3,*], Marcelo A. S. de Toledo[1,2], Janik Böhnke[4,5], Martin Graßhoff[6], Ivan G. Costa[6] , Alexandre Theocharides[7], Angela Maurer[1,2], Herdit M. Schüler[8], Eva Miriam Buhl[9], Kristina Pannen[1,2], Julian Baumeister[1,2], Milena Kalmer[1,2], Siddharth Gupta[1,2], Peter Boor[9], Deniz Gezer[1,2], Tim H. Brümmendorf[1,2], Martin Zenke[4,5], Nicolas Chatain[1,2,#] & Steffen Koschmieder[1,2,#]

[1]Department of Hematology, Oncology, Hemostaseology, and Stem Cell Transplantation, Faculty of Medicine, RWTH Aachen University, Aachen, Germany

[2]Center for Integrated Oncology Aachen Bonn Cologne Düsseldorf (CIO ABCD)

[3]Department of Oncology, The First Affiliated Hospital of Zhengzhou University, Zhengzhou, China

[4]Institute for Biomedical Engineering, Department of Cell Biology, Faculty of Medicine, RWTH Aachen University, Aachen, Germany

[5]Helmholtz Institute for Biomedical Engineering, RWTH Aachen University, Aachen, Germany

[6]Institute for Computational Genomics Joint Research Center for Computational Biomedicine, Faculty of Medicine, RWTH Aachen University, Aachen, Germany

[7]Division of Hematology, University Hospital Zurich and University of Zurich, Zurich, Switzerland

[8]Institute for Human Genetics, Faculty of Medicine, RWTH Aachen University, Aachen, Germany

[9]Institute for Pathology, Electron Microscopy Facility, Faculty of Medicine, RWTH Aachen University, Aachen, Germany

[*]These authors contributed equally

[#]Co-senior authors

Correspondence: Prof. Dr. med. Steffen Koschmieder, Department of Hematology, Oncology, Hemostaseology, and Stem Cell Transplantation, Faculty of Medicine, RWTH Aachen University, Pauwelsstr. 30, D-52074 Aachen, Germany, Phone: +49-241-8036102; E-mail: skoschmieder@ukaachen.de

Supplemental Information

1. Supplemental Figures

Figure S1. Proof of CRISPR/Cas9 engineered *CALR* WT clones.

Figure S2. Gating strategy and impact of CALR mutations on HSPCs proliferation

Figure S3. Impact of CALR mutations on MKs proliferation capacity and on erythrocytic cell development

Figure S4. Immunofluorescence staining to determine wild type and mutant CALR distribution in the cell

Figure S5. Gene ontology (GO) analysis of *CALR*ins5-mutated iPSC-derived MKs

2. Supplemental Tables

Table S1. Generation of MPN patient-derived CALR iPSCs

Table S2. CRISPR guide RNAs (gRNAs) to repair homozygous CALR mutations with CRISPR/Cas9

Table S3. Donor template to repair homozygous CALR mutations with CRISPR/Cas9

Table S4. NGS Data of patient-derived CALR iPSCs and Healthy donor

Table S5. List of antibodies used for flow cytometry

Table S6. List of primary and secondary antibodies used for Western blot and Immunofluorescence

Table S7. List of primers used for RT-qPCR and CALR genotyping PCR

Table S8. Medium composition

3. Supplemental Experimental Procedures

-Next generation sequencing

-Cytogenetic analysis

-Immunofluorescence staining

-RNA isolation and RT-qPCR

-SDS-Page and Western blot

-Undirected hematopoietic differentiation of iPSCs into hematopoietic progenitors and myeloid subsets with the “EB-based” protocol

-Differentiation of iPSCs into hematopoietic stem cells and myeloid subsets with the “spin-EB” protocol

-Cell morphology analysis

-MPO cytochemical staining

-Flow cytometry analysis

-CRISPR/Cas9-mediated repair of homozygous *CALRins5* and *CALRdel52* mutation in iPSCs

-Purification of CD34+ HSPCs and CD61+ megakaryocytes by magnetic activated cell sorting

-Colony-forming unit assay of CD34+ HSPCs

-Transmission electron microscopy

-Preparation of samples for RNA Sequencing

1. Supplemental Figures

Figure S1.

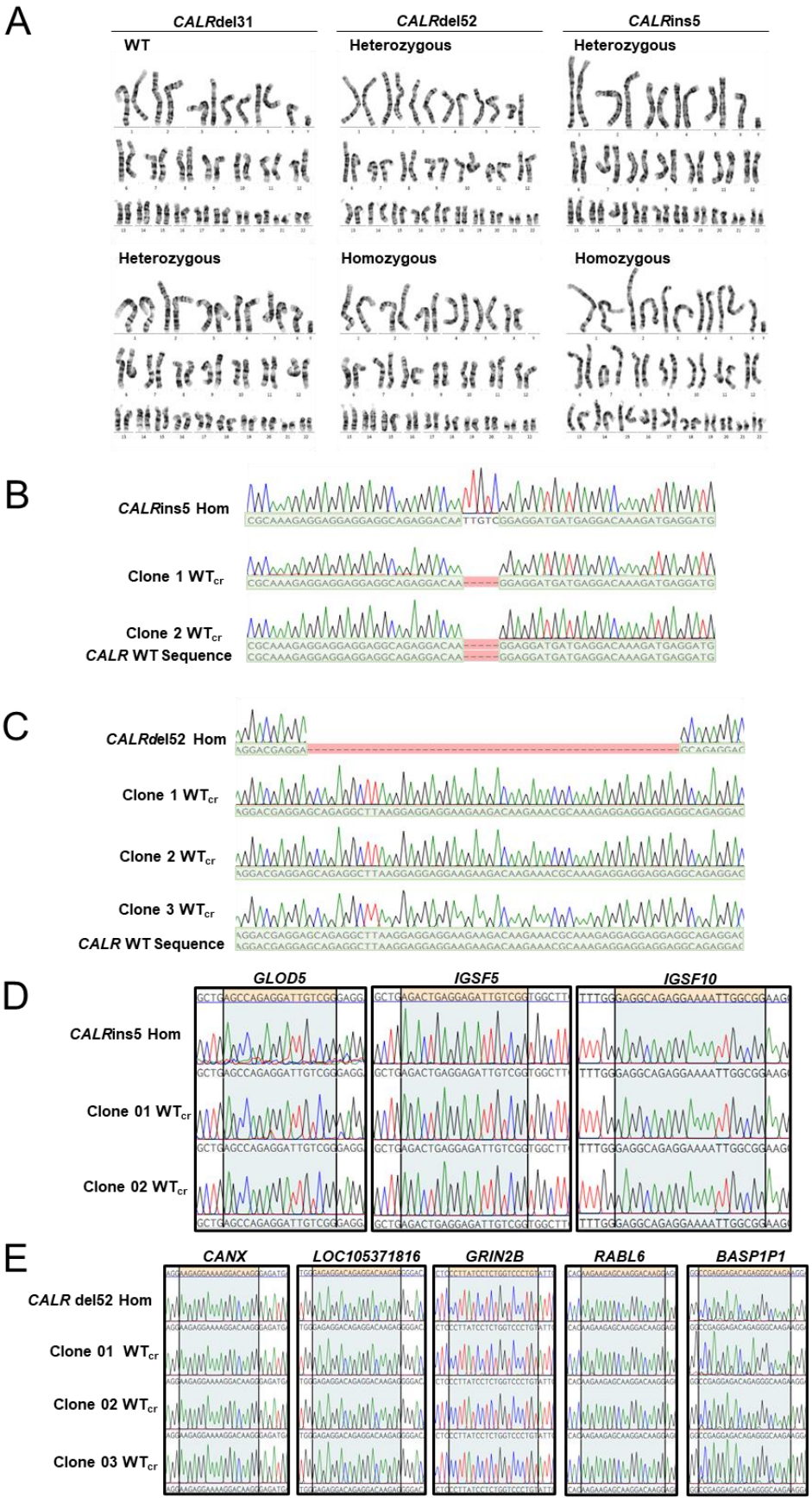

Figure S1. Proof of CRISPR/Cas9 engineered *CALR* WT clones. Related to Figure 1.

A. Karyotype analysis of patient-derived iPSC clones. **B.** Sequence alignment of maternal homozygous *CALR*ins5 clone with resulting WT_{cr} clones 01 and 02 to reference CALR WT sequence. Successful alignment and mismatch are shown in green and red, respectively. **C.** Sequence alignment of maternal homozygous *CALR*del52 clone with resulting WT_{cr} clones 01, 02, and 03 to reference CALR WT sequence. Successful alignment and mismatch are shown in green and red, respectively. **D.** and **E.** Exclusion of possible off-target effects caused by CRISPR/Cas9 gene editing for *CALR* mutations. List of off-targets was provided by IDT Systems. To verify off-target sites, regions of interest were amplified by PCR and Sanger sequenced. Sequence alignment of maternal homozygous *CALR*ins5 clone (**D**) and resulting WT_{cr} clones 01 and 02 for possible off-targets in *GLOD5*, *IGSF5,* and *IGSF10*. Regions of interest are highlighted in orange/grey. Sequence alignment of maternal homozygous *CALR*del52 clone (**E**) and resulting WT_{cr} clones 01, 02, and 03 for possible off-targets in *CANX*, *LOC105371816, GRIN2B, RABL6,* and *BASP1P1*. Regions of interest are highlighted in orange/grey.

Figure S2.

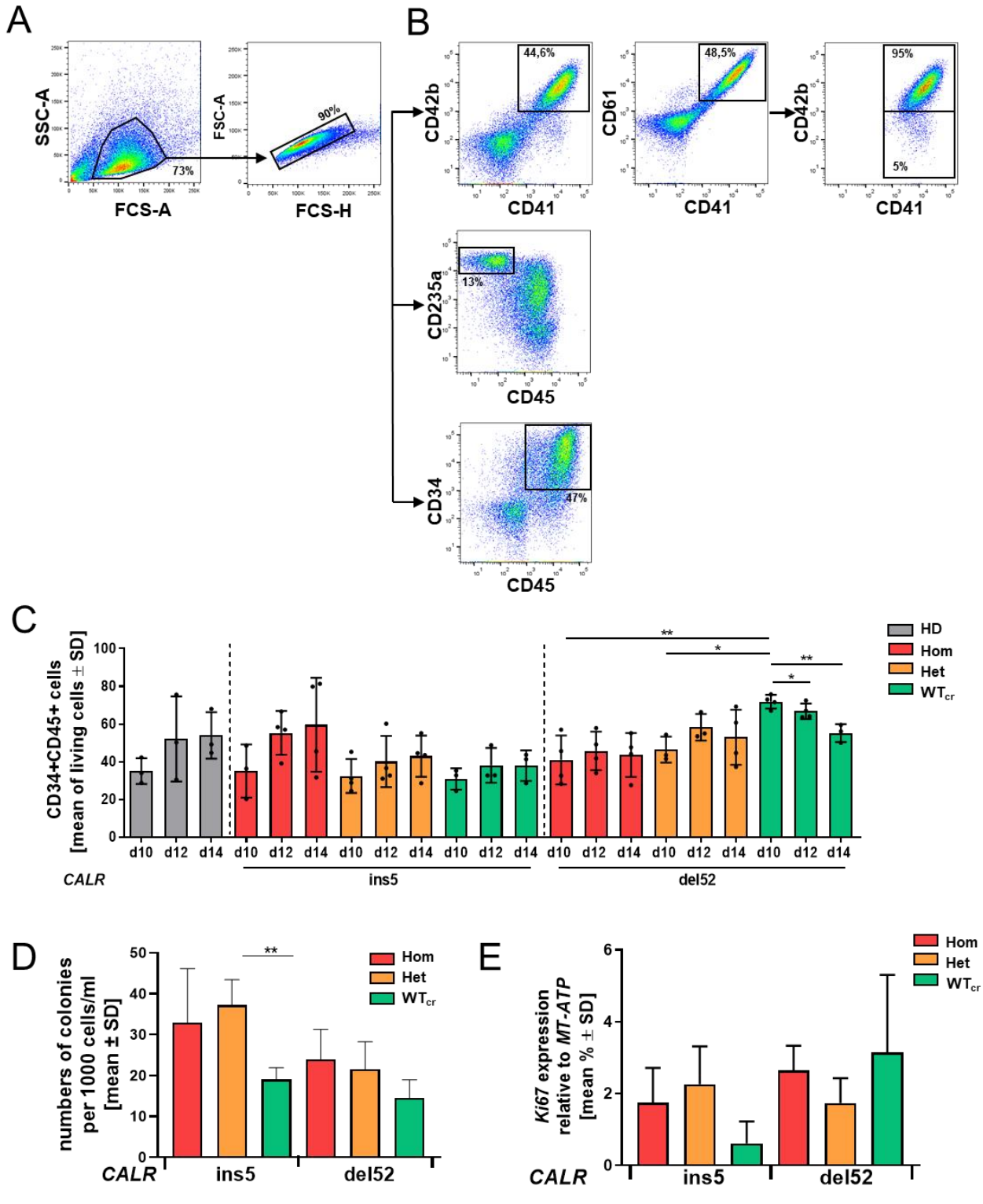
A
SSC-A
FCS-A
73%
FSC-A
FCS-H
90%
B
CD42b
CD41
44,6%
CD61
CD41
48,5%
CD42b
CD41
95%
5%
CD235a
CD45
13%
CD34
CD45
47%
C
CD34+CD45+ cells
[mean of living cells ± SD]
HD
Hom
Het
WTcr
d10 d12 d14 d10 d12 d14 d10 d12 d14 d10 d12 d14 d10 d12 d14 d10 d12 d14 d10 d12 d14
CALR
ins5
del52
D
numbers of colonies
per 1000 cells/ml
[mean ± SD]
Hom
Het
WTcr
CALR
ins5
del52
E
Ki67 expression
relative to MT-ATP
[mean % ± SD]
Hom
Het
WTcr
CALR
ins5
del52

Figure S2. Gating strategy and impact of CALR mutations on HSPCs proliferation. Related to Figure 3 and Figure 4.

A. Flow cytometry analysis gating strategy to identify myeloid cell populations in „spin-EB“ differentiation protocol. Living cells were first gated on forwards scatter (FSC-A)/side scatter (SSC-A) and further gated on single cells. **B.** Mature and immature MKs were identified by CD42b+CD41+ and CD61+CD41+, respectively. Erythroid cells were discriminated by CD235a+CD45- expression and HSPCs were determined by CD34+CD45+ expression. Numbers represent frequencies of indicated populations in percentage of living cells. **C.** Percentage of CD34+CD45+ cells on day 10, day 12 and day 14 of „spin-EB“ differentiation analyzed by flow cytometry analysis. Each data point represents an independent experiment for each *CALR* genotype and HD control shown as mean values ± SD, **p*<0.05, ***p*<0.01, *n*=3-4 independent experiments. **D.** Number of colonies counted from colony forming unit assay. Statistics was calculated by comparing mutated cells to corresponding WT_{cr} cells. Data are shown as mean values ± SD, ***p*>0.01, *n*=3-5 independent differentiation experiments. **E.** Gene expression of the proliferative marker *Ki67* measured in iPS-derived HSPC in RT-qPCR. Data are shown for three independent experiments (*n*=3) with indicated CALR genotype. Gene expression was normalized to *MT-ATP6* expression and is represented as mean values ± SD.

Figure S3.

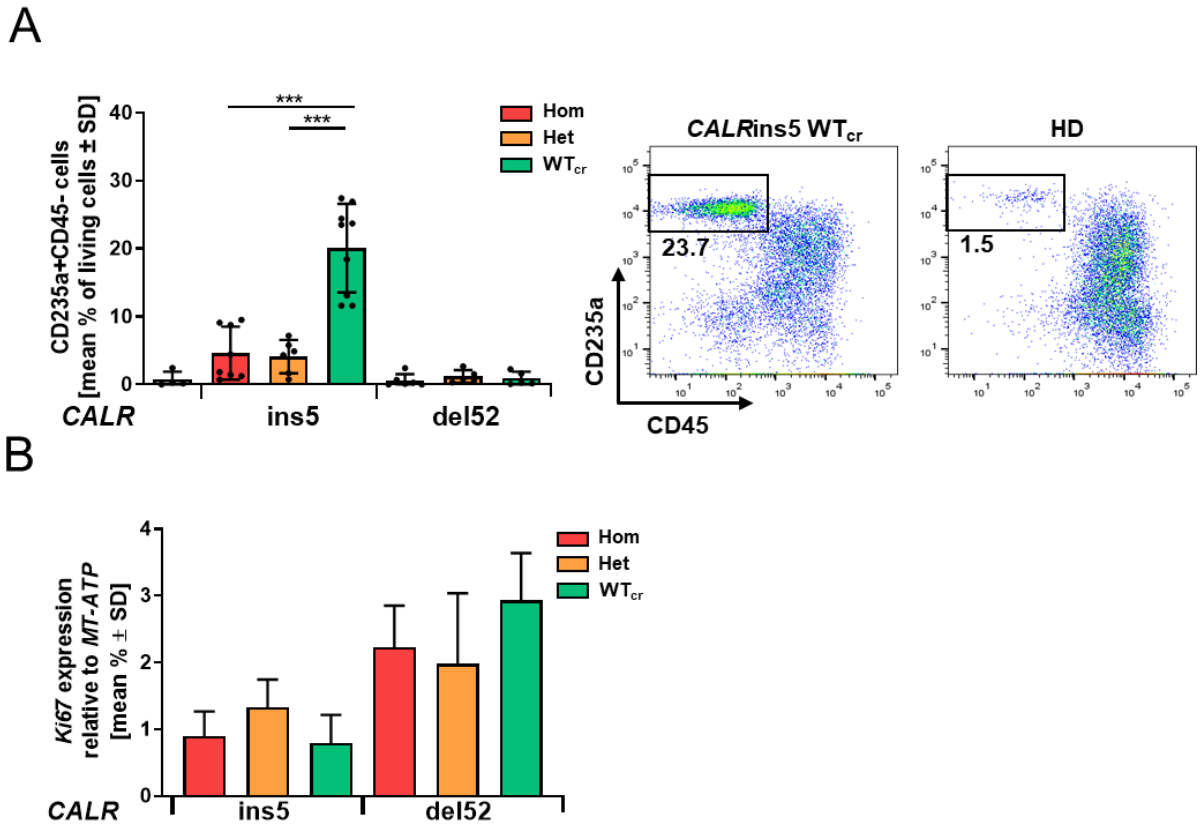

Figure S3.Impact of CALR mutations on MKs proliferation capacity and on erythrocytic cell development. Related to Figure 4.

A. Percentage of CD235a+CD45- erythroid cells determined by flow cytometry on day 14 of "spin-EB" differentiation. Number of independent experiments performed for each *CALR* genotype and HD control referred to number of data points shown, *n*=4-9. Flow cytometry plots to determine erythroid cell population (CD235a+CD45-) are exemplarily shown for *CALR*ins5 WT_{cr} cells and healthy controls. Numbers represent frequencies of indicated populations in percentage of living cells as mean values ± SD. ***p<0.001. **B.** Gene expression of the proliferative marker *Ki67* measured in iPS-derived MKs in RT-qPCR. Data are shown for three independent experiments (*n*=3) with indicated CALR genotype. Gene expression was normalized to *MT-ATP6* expression and are shown as mean values ± SD.

Figure S4.

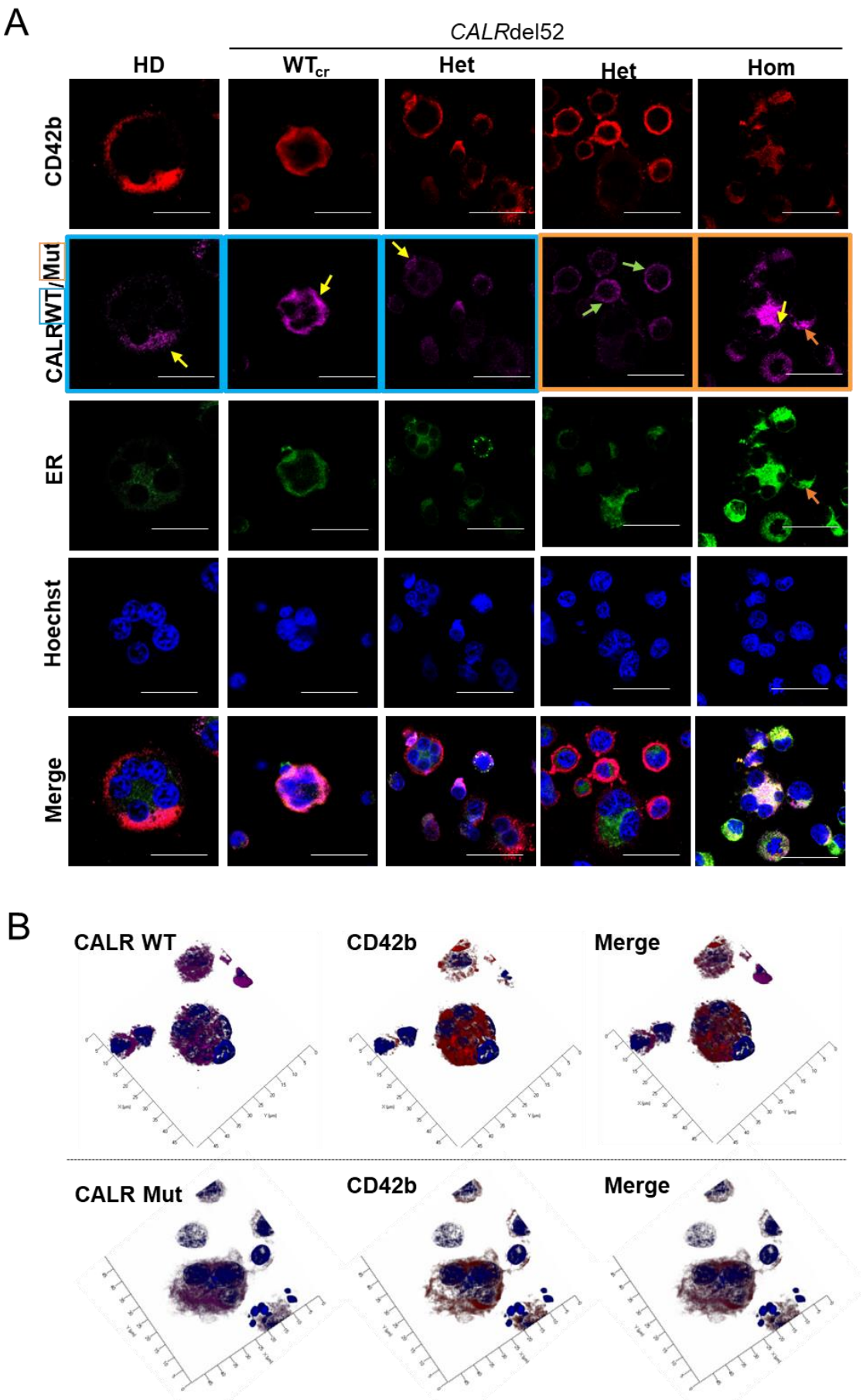
A
CALRdel52
HD
WTcr
Het
Het
Hom
CD42b
CALRWT/Mut
ER
Hoechst
Merge
B
CALR WT
CD42b
Merge
CALR Mut
CD42b
Merge

Figure S4. Immunofluorescence staining to determine wild type and mutant CALR distribution in the cell. Related to Figure 6.

A. iPSC-derived MKs were fixed and stained for the endoplasmic reticulum (ER) and wild type (WT) CALR or mutated (Mut) CALR, indicated with blue or orange frames, respectively, after 14 days of differentiation for indicated iPSC clones. To identify MKs, samples were additionally stained for CD42b. Hoechst was added for nuclear staining. Scale bars, 50 µm. Diffuse CALR distribution, clustered localization of CALR at the cell surface, and co-localization of CALR and ER are indicated with yellow, green, and orange arrows, respectively. **B.** Z-stack images of heterozygous *CALR*ins5-mutated MKs for indicated staining. Hoechst was added for nuclear staining. Scale bars, 50 µm.

Figure S5.

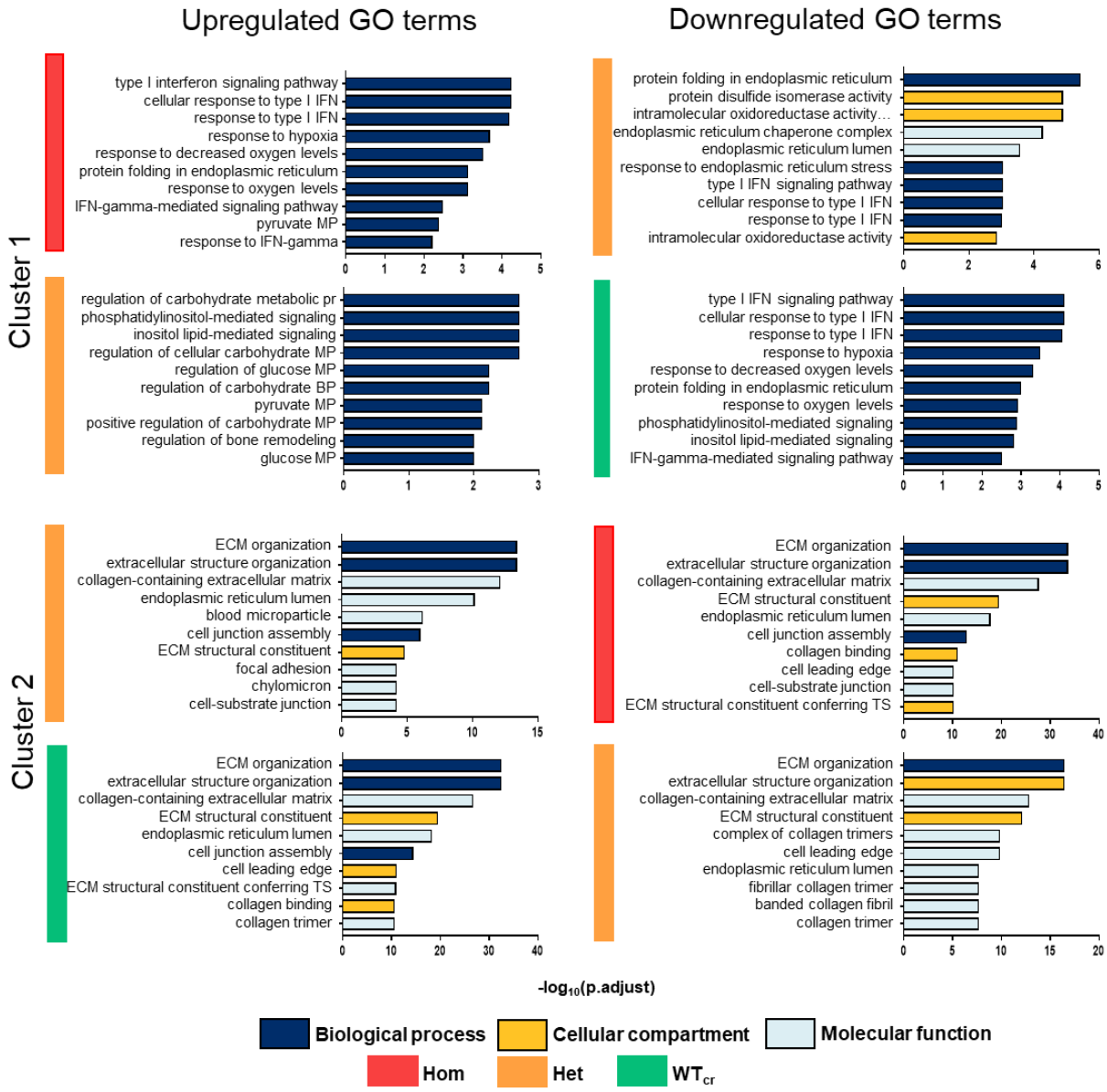
Upregulated GO terms
Downregulated GO terms
Cluster 1
Cluster 2
type I interferon signaling pathway
cellular response to type I IFN
response to type I IFN
response to hypoxia
response to decreased oxygen levels
protein folding in endoplasmic reticulum
response to oxygen levels
IFN-gamma-mediated signaling pathway
pyruvate MP
response to IFN-gamma
protein folding in endoplasmic reticulum
protein disulfide isomerase activity
intramolecular oxidoreductase activity…
endoplasmic reticulum chaperone complex
endoplasmic reticulum lumen
response to endoplasmic reticulum stress
type I IFN signaling pathway
cellular response to type I IFN
response to type I IFN
intramolecular oxidoreductase activity
regulation of carbohydrate metabolic pr
phosphatidylinositol-mediated signaling
inositol lipid-mediated signaling
regulation of cellular carbohydrate MP
regulation of glucose MP
regulation of carbohydrate BP
pyruvate MP
positive regulation of carbohydrate MP
regulation of bone remodeling
glucose MP
type I IFN signaling pathway
cellular response to type I IFN
response to type I IFN
response to hypoxia
response to decreased oxygen levels
protein folding in endoplasmic reticulum
response to oxygen levels
phosphatidylinositol-mediated signaling
inositol lipid-mediated signaling
IFN-gamma-mediated signaling pathway
ECM organization
extracellular structure organization
collagen-containing extracellular matrix
endoplasmic reticulum lumen
blood microparticle
cell junction assembly
ECM structural constituent
focal adhesion
chylomicron
cell-substrate junction
ECM organization
extracellular structure organization
collagen-containing extracellular matrix
ECM structural constituent
endoplasmic reticulum lumen
cell junction assembly
collagen binding
cell leading edge
cell-substrate junction
ECM structural constituent conferring TS
ECM organization
extracellular structure organization
collagen-containing extracellular matrix
ECM structural constituent
endoplasmic reticulum lumen
cell junction assembly
cell leading edge
ECM structural constituent conferring TS
collagen binding
collagen trimer
ECM organization
extracellular structure organization
collagen-containing extracellular matrix
ECM structural constituent
complex of collagen trimers
cell leading edge
endoplasmic reticulum lumen
fibrillar collagen trimer
banded collagen fibril
collagen trimer
-log10(p.adjust)
Biological process
Cellular compartment
Molecular function
Hom
Het
WTcr

Figure S5. Gene ontology (GO) analysis of *CALR*ins5-mutated iPSC-derived MKs. Related to Figure 7.

Gene ontology (GO) analysis based on up- and downregulated genes of cluster-wise analysis for the heat map (Figure 7A) shown in the main text. The top 10 GO terms are shown. GO categories biological process, cellular compartment and molecular functions are depicted in dark blue, yellow, and light blue, respectively. Corresponding genotypes are shown in red, orange and green for MKs with homozygous (Hom) or heterozygous (Het) *CALR*ins5, or WT_{cr} MKs, respectively. BP (biosynthetic process), ECM (extracellular matrix), MP (metabolic process), TS (tensile strength), IFN (interferon).

Figure S6.

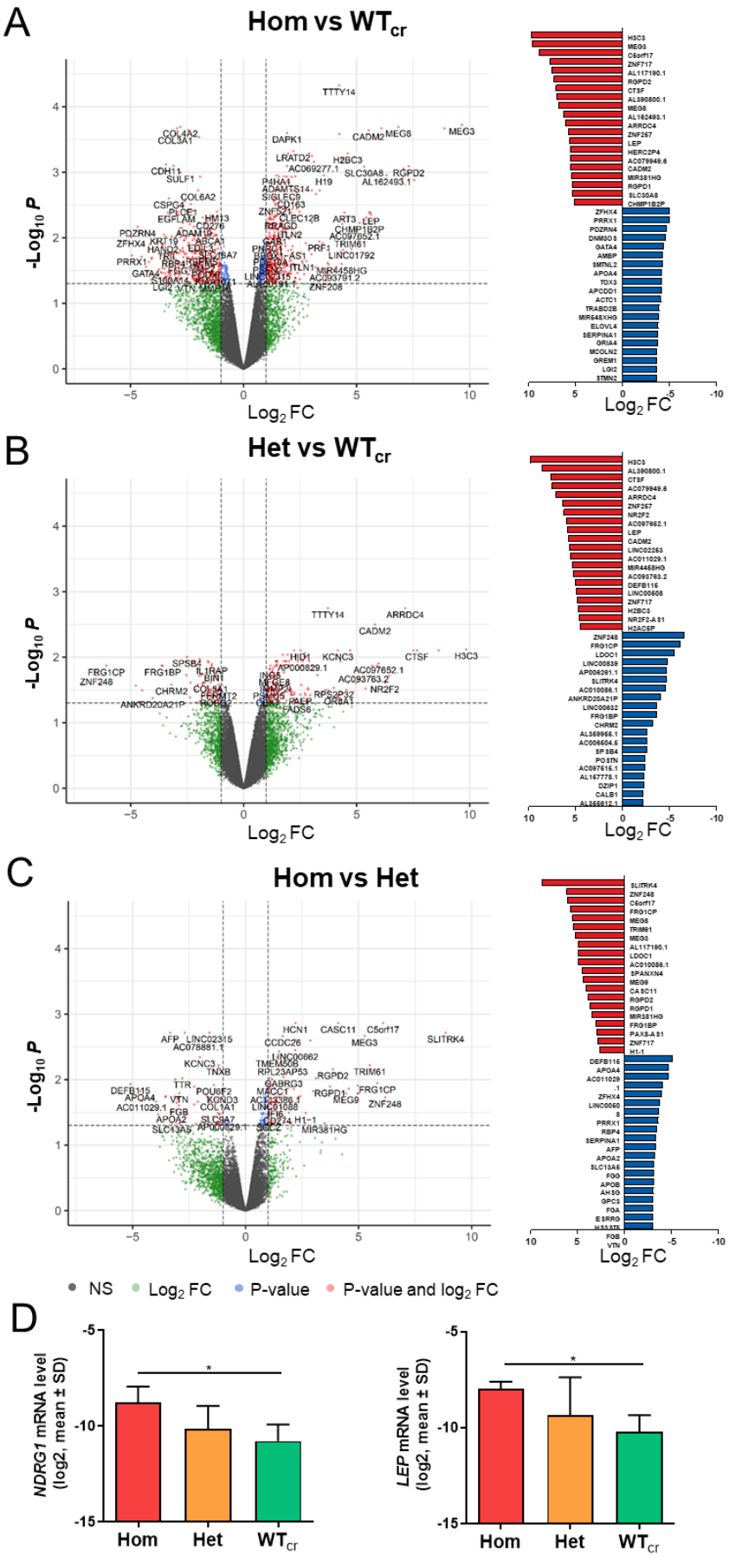
A
Hom vs WTcr
B
Het vs WTcr
C
Hom vs Het
-Log10 P
Log2 FC
NS
Log2 FC
P-value
P-value and log2 FC
D
NDRG1 mRNA level (log2, mean ± SD)
LEP mRNA level (log2, mean ± SD)
Hom
Het
WTcr

Figure S6. Differentially expressed genes (DEGs) in *CALR*ins5-mutated MKs and WT_{cr} MKs. Related to Figure 7.

A., **B.**, and **C**. Volcano plot of differentially expressed genes (DEGs) and list of the top 20 up- and downregulated DEGs among the comparisons: Hom vs WT_{cr} (**A**), Het vs WT_{cr} (**B**), and Hom vs Het (**C**) of CALRins5-muated MKs and control. All genes shown in the list of DEGs are significantly regulated (p≤0.05) Up-and downregulated genes are shown in red and blue, respectively. FC (fold change), Hom (homozygously *CALR*ins5-mutated), Het (heterozygously *CALR*ins5-mutated). **D.** Validation of RNAseq analysis by RT-qPCR for *NDRG1* and leptin (*LEP*) expression. RT-qPCR was performed for two samples also analyzed in RNAseq and one sample from an additional independent differentiation experiment, *n*=3 independent experiments, **p*<0.05. Hom (homozygously *CALR*ins5-mutated), Het (heterozygously *CALR*ins5-mutated).

3. Supplemental Tables

Table S1. Generation of MPN patient-derived CALR iPSCs

Pat.	Diagnosis	CALR mutation	Sample type	Allele burden	iPS clones screened	CALR non-mut clones	CALR Heterozygous clones	CALR homozygous clones
1	pET-MF	ins5	PB	82%	101	0	27	74
2	PMF	del52	PB	51%	64	0	55	9
3	PMF	del31	PB	37%	69	5	64	0

Table S1. iPSCs were generated by reprogramming peripheral blood-derived mononuclear cells from three patients carrying *CALR* del52, ins5, or del31 mutation. Individual colonies were picked and screened for *CALR* genotypes by PCR. Abbreviations: CALR, calreticulin; iPSC, induced pluripotent stem cell; non-mut, non-mutant; PMF, primary myelofibrosis; pET-MF, secondary post essential thrombocythemia myelofibrosis. PB, peripheral blood.

Table S2. CRISPR guide RNAs (gRNAs) to repair homozygous CALR mutations with CRISPR/Cas9. Related to Figure 1.

Mutation	gRNA
*CALR*ins5	5'-AGGCAGAGGACAATTGTCGG -3'
*CALR*del52	5'-ACGAGGAGCAGAGGACAAGG-3'

Table S3. Donor template to repair homozygous CALR mutations with CRISPR/Cas9. Related to Figure 1.

Mutation	Donor Template
*CALR*ins5	5'- GAGGCTTAAGGAGGAGGAAGAAGACAAGAAACGCAAAGAGGAGGA GGAGGCAGAGGACAAGGAGGATGATGAGGACAAAGATGAGGATGA GGAGGATGAGGAGGACAAGGAGGAAGATGA -3'
*CALR*del52	5'- GTGCTCTGCCTGCAGGCAGCAGAGAAACAAATGAAGGACAAACAG GACGAGGAGCAGAGGCTTAAGGAGGAGGAAGAAGACAAGAAACGC AAAGAGGAGGAGGAGGCAGAGGACAAGGAGGATGATGAGGACAAA GATGAGGATGAGGAGGATGAGGAGGACAAGGAGGAAG -3'

Table S4. NGS Data of patient-derived CALR iPSCs and Healthy donor

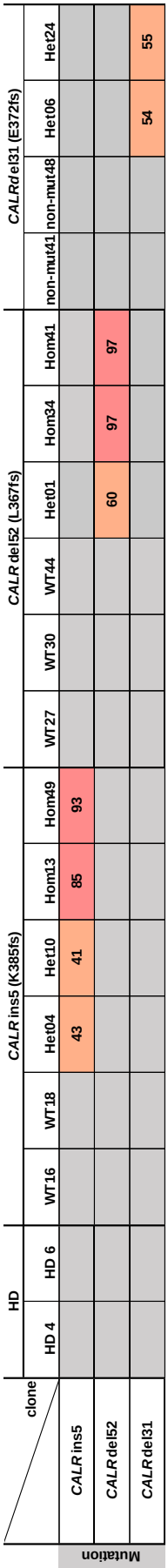

Table S4. Next generation sequencing (NGS) of patient-derived iPSC clones and healthy donors iPSC clones for clinically relevant MPN mutations. In the analyzed gene list (*ABL1, ASXL1, BRAF, BTK, CBL, CSF3R, CXCR4, DNMT3A, ETNK1, EZH2, FLT3, IDH1, IDH2, JAK2, KIT, KRAS, MPL, MYD88, NF-E2, NPM1, NRAS, PTPN11, RUNX1, SETBP1, SF3B1, SH2B3, STAT5B, TET2, TP53, U2AF1, WT1)* no mutation was found. Percentages represent allele frequency (the fraction of mutant reads per total reads) of indicated mutations.

Table S5. List of antibodies used for flow cytometry. Related to Figure 2 and Figure 4.

Antibody	**Company**	**Catalogue number**
APC mouse anti-human CD34	BD, USA	555824
FITC mouse anti-human CD43	BD, USA	555475
PE mouse anti-human CD31	BD, USA	555446
FITC anti-human CD61 clone VI-PL2	BioLegend, USA	336404
Anti-human CD117 (ckit)-PE Cy7 clone 104D2	Thermo Fisher Scientific, USA	25-1178-42
Anti-human CD235a-PE clone HIR2	Thermo Fisher Scientific, USA	12-9987-82
CD45-APC-Vio770 human	Miltenyi Biotec, Germany	130-113-115
APC anti-human CD42b	BioLegend, USA	303912
PE/Cyanina7 anti-human CD41	BioLegend, USA	303718
CD45-APC human	Beckman Coulter. USA	IM2473U
CD15-PC5 human	Beckman Coulter, USA	B49217
MPO-FITC human	Beckman Coulter, USA	IM1874

Table S6. List of primary and secondary antibodies used for Western blot and Immunofluorescence. Related to Figure 1 and Figure 6.

Antibody	**Company**	**Catalogue number**
Monoclonal anti-mutated Calreticulin Rabbit	Dianova, Germany	DIA-CAL-250
Monoclonal anti Calreticulin (D3E6) XP Rabbit #12238	Cell Signaling, USA	12238S
Monoclonal GAPDH (0411): sc-32233 Mouse	Santa Cruz Biotechnology, USA	sc-47724
CD42b Polyclonal Antibody	Thermo Fisher Scientific, USA	PA5-90903
Calreticulin Antibody (1G6A7)	Novus Biologicals, USA	47518SS
Goat anti-rabbit IgG (H+L) Alexa Fluor 555	Thermo Fisher Scientific, USA	A32732
Goat anti-mouse IgG (H+L) Alexa Fluor 647	Thermo Fisher Scientific, USA	A32728

Goat anti-rabbit IgG (H+L) FITC	Thermo Fisher Scientific, USA	F-2765
Goat anti-mouse IgM (H+L) Alexa Fluor 594	Thermo Fisher Scientific, USA	A-11012
Goat anti-mouse Immunoglobulins/HRP, polyclonal	Dako, USA	P0447
Goat anti-rabbit Immunoglobulins/HRP, polyclonal	Dako, USA	P0448

Table S7. List of primers used for qPCR and CALR genotyping PCR. Related to Figure 1, Figure 5 and Figure S1.

Target name		Sequence	Reference
qPCR			
*CALR*del52	Non-.mut allele FRW	CAGGACGAGGAGCAGAGACT	
	Mutant allele FRW	ACAGGACGAGGAGCAGAGAAC	
	Common Rev	GCCTCTCTACAGCTCGTCCTTG	
*CALR*del31	Non-.mut allele FRW	CAAGTCTGGCACCATCTTTG	
	Mutant allele FRW	TCCTCTTTGCGTTTCTTGTC	
	Common Rev	ATCCTCCTTGTCCTCTGTTC	
*CALR*ins5	common FRW	CAAGTCTGGCACCATCTTTG	
	Non-mut allele Rev	TGTCCTCATCATCCTCCTTG	
	mutant Rev	TGTCCTCATCATCCTCCGAC	
ETS1	FRW	TCGATCTCAAGCCGACTCTC	
	REV	CATTCACAGCCCACATCACC	
FLI1	FRW	GTGCTGTTGTCACACCTCAG	
	REV	TACTGATCGTTTGTGCCCCT	
GAPDH	FRW	GTTGAGGTCAATGAAGGGGTC	
	REV	GACCTCAACTACATGGTGAGTTGC	
GATA1	FRW	GGGATCACACTGAGCTTGC	(Szabo et al., 2010)
	REV	ACCCCTGATTCTGGTGTGG	
GFI1B	FRW	AGTTCTGCGGCAAGCGTTTCCA	
	REV	TTTCCGCACACCTGGCACTTGT	
Ki67	FRW	CAGACCCATTTACTTGTGTTGGA	
	REV	ACGCCTGGTTACTATCAAAAGG	
LEP	FRW	CGGTAAGGAGAGTATGCGGG	
	REV	ACCAGAAAGAGTGGAGCCT	
LOX1	FRW	GCATACAGGGCAGATGTCAGA	
	REV	TTGGCATCAAGCAGGTCATAG	
MPL	FRW	CTGCCACTTCAAGTCACGAA	
	REV	CTGCCACTCCAATTCCAGAT	
MPO	FRW	CCGGGATGGTGATCGGTTTT	(Theocharides et al., 2016)
	REV	CAGATGATCCGGGGCAATGA	
MT-ATP6	FRW	CGTACGCCTAACCGCTAACA	
	REV	AGGCGACAGCGATTTCTAGG	
NRDG1	FRW	GACAAAGGCCAAAAGGTCAACA	

	REV	CCATTTCATTGGGAGGGTGGT	
NFE2	FRW	CTGTGACTCCACCACAGGTTT	
	REV	TGAGCAGGGGCAGTAAGTTG	
RUNX1	FRW	CCGAGAACCTCGAAGACATC	
	REV	GTCTGACCCTCATGGCTGT	
vWF	FRW	CAACACCTGCATTTGCCGAA	
	REV	TGACCTGTGACAAGGCACTC	
Genotyping PCR			
*CALR*del52 r	FRW	ACAACTTCCTCATCACCAACG	
*CALR*del31	REV	GGCCTCAGTCCAGCCCTG	
Gentoyping allele specific PCR			
*CALR*ins5	common FRW	TAACTGCAGTGTCAGCGGTG	
	Non-mut allele Rev	TGTCCTCATCATCCTCCTTG	
	mutant Rev	TGTCCTCATCATCCTCCGAC	
PCR for CRISPR-off target products			
CANX	FRW	ACACGTCTTCAGGGTAGGA	
	REV	CAACATCGTAGGGTCTTGGCT	
RABL6	FRW	GCAAAGAGGTACTGGCTACTCC	
	REV	CGGCCTAGAGCTCCTCGTA	
BASP1P1	FRW	GGCGGAGCTAGCACTACAAC	
	REV	GGTGACTTCGGCAGCTTTGG	
IGSF10	FRW	AAGTGAGTGAACCCAGGCAC	
	REV	AGCTTTGGGGAAGGTGATGG	
IGSF5	FRW	TAGAGATTCCTGGTTCCTGGG	
	REV	TCCACCGCCACGTCCTAGATT	
GRIN2B	FRW	TCACCACACACGCTACTTCCAC	
	REV	TTTACAGAGAAGGCTGGCCG	
GLOD5	FRW	CCTTCCATTTGCACTACCTACCT	
	REV	CCCTGGCTAAACTGGGGGAG	
LOC105371816	FRW	TCTTGGAGACAGACTGCTGG	
	REV	GTGTGGGGTCCTGATGCTTTA	

Table S8. Medium composition. Related to Figure 2, Figure 3 and Figure 4.

SFM Medium for "spin-EB" differentiation		
50 %	IMDM	Thermo Fisher Scientific, USA
50 %	Ham's F-12 Nutrient Mixture	Thermo Fisher Scientific, USA
0.5 %	Human Plasbumin 20	Grifols, Germany
2 mM	GlutaMAX	Thermo Fisher Scientific, USA
2 mM	Chemically Defined Lipid Concentrate	Thermo Fisher Scientific, USA
50 µg/ml	L-ascorbic acid	Stemcell Technologies, Canada
6 µg/ml	Transferrin	Merck, Germany
400 µM	1-Thioglycerol	Merck, Germany

EB medium for EB-based differentiation		
	IMDM	Thermo Fisher Scientific, USA
15 %	FBS	Pan Biotech, Germany
1U/ml	Penicillin	Thermo Fisher Scientific, USA
100 mg/ml	Streptomycin	Thermo Fisher Scientific, USA
2 mM	L-Glutamine	Thermo Fisher Scientific, USA
5 %	Protein-Free Hybridoma Medium-II	Thermo Fisher Scientific, USA

0.1 mM	β-mercaptoethanol	Thermo Fisher Scientific, USA
50 µg/ml	L-Ascorbic acid	Sigma Aldrich, Germany
175 µg/ml	hTransferrin	Sigma Aldrich, Germany

Progenitor medium for EB-based differentiation		
	StemPro 34 SFM	Thermo Fisher Scientific, USA
2 mM	L-Glutamine	Thermo Fisher Scientific, USA
1U/ml	Penicillin	Thermo Fisher Scientific, USA
100 mg/ml	Streptomycin	Thermo Fisher Scientific, USA
1X	MEM Non-Essential Amino Acids	Thermo Fisher Scientific, USA

3. Supplemental experimental procedures

Next generation sequencing

For the detection of mutations from gDNA by next generation sequencing (NGS), two panels individually designed and validated for routine hematology diagnostic were used. Either 250ng or 75ng of gDNA were used for library preparation with either a Truseq Custom Amplicon Kit (Illumina, San Diego, USA) or an Ampliseq for Illumina Custom Panel (Illumina) covering the relevant regions of either 31 (*ABL1, ASXL1, BARD1, CALR, CBL, CHEK2, CSF3R, DNMT3A, ETNK1, ETV6, EZH2, IDH1, IDH2, JAK2, KIT, KRAS, MPL, NFE2, NRAS, PDGFRA, PTPN11, RUNX1, SETBP1, SF3A1, SF3B1, SH2B3 (LNK), SRSF2, TCF12, TET2, TP53, U2AF1*)(Kirschner et al., 2018) or 32 genes (*ABL1, ASXL1, BRAF, BTK, CALR, CBL, CSF3R, CXCR4, DNMT3A, ETNK1, EZH2, FLT3, IDH1, IDH2, JAK2, KIT, KRAS, MPL, MYD88, NF-E2, NPM1, NRAS, PTPN11, RUNX1, SETBP1, SF3B1, SH2B3, STAT5B, TET2, TP53, U2AF1, WT1*) associated with hematologic malignancies. The final libraries were sequenced with 2x250bp on a MiSeq (Illumina). The MiSeq onboard software was used (Real time analysis software v1.18.54, Illumina) for demultiplexing and FastQ file generation. Alignment and variant calling were performed with the SeqNext-Module of the SeqPilot-Software (JSI medical systems, Version 4.4.0 Build 509). Variants were called with a bidirectional frequency of >5% (JAK2 V617F and KIT D816V >1%) and reviewed manually.

Cytogenetic analysis

Patient-derived iPSC clones were seeded on matrigel coated 25 cm^2 cell culture flasks. Normal chromosomal constitution was verified by conventional karyotyping of iPSC clones by means of GTG banding at 400 to 550 band level. Metaphase spreads were prepared using standard procedures of blocking cell division at metaphase, hypotonic treatment, and methanol/acetic acid fixation (3:1). The banding techniques included the use of a trypsin pretreatment (GTG-banding) carried out according to standard protocols. Microscopy was performed with Axioplan fluorescence microscope (Carl Zeiss) and IKARUSTM digital imaging systems (MetaSystems, Altlussheim, Germany). An average of 20 mitoses were analyzed for each clone.

Immunofluorescence staining

iPSC colonies were cultured on Matrigel coated coverslips in 4-well-plates. Cells were fixed with 4 % paraformaldehyde (Sigma Aldrich) and blocked with goat serum (Merck Millipore, Darmstadt, Germany). In order to detect the expression of pluripotent markers and mutant CALR, cells were incubated with following primary antibodies at 4 °C overnight: TRA-1-60 (Merck Millipore), OCT3/4 (H-134, Santa Cruz, CA, USA) or mouse monoclonal antibody CAL2 (Dianova, Hamburg, Germany). Cells were washed three times with PBS on the next day and

incubated with corresponding secondary antibodies goat anti-rabbit IgG (H+L) FITC (Thermo Fisher Scientific), goat anti-mouse IgM (H) Alexa Fluor 594 (Thermo Fisher Scientific) or goat anti-mouse IgG Alexa Fluor 647 (for CALR mutant, clone poly4053, BioLegend, San Diego, CA, USA) for 1 h in the dark. Nuclei were stained with DAPI (Vector Laboratories, Burlingame, CA, USA) and coverslips were mounted with Dako Fluorescence Mounting Medium (Dako, Jena, Germany). Fluorescent image analysis was performed using an Axiovert 200 microscope (Carl Zeiss, Jena, Germany) and IPLab Spectrum software (BD, Franklin Lakes, USA).

In order to detect localization of WT and mutand CALR in MKs, cells were fixed with 3,7 % PFA, washed with PBS and permeabilized with 0,1 % Trition-X and 2,5 % BSA. Afterwards cells were incubated with detection reagent for ER-staining and Hoechst (Enzo Life Sciences, Farmingdale,USA) for 20 min at 37°C. Cells were washed with PBS and blocked wit 5 % BSA in PBS. Cells were incubated with the following primary antibodies at 4 °C overnight: polyclonal antibody CD42b (Thermo Fisher Scientific) and mutant CALR antibody (Dianova) or WT CALR monoclonal antibody (Novus, Littleton, USA). On the next day, cells were washed with PBS and incubated with corresponding secondary antibodies goat anti-rabbit IgG Alexa Fluor 555 (H+L) and goat anti-mouse IgG (H+L) Alexa Fluor 647(all Thermo Fisher Scientific) for 1 h at RT. Coverslips were mounted with Fluorescence Mounting Medium (Dako, Carpinteria, USA). Fluorescent image analysis was performed using a confocal Scanning Microscope (LSM 710) microscope and Zeiss 2012 software (both Carl Zeiss, Jena, Germany).

RNA isolation and RT-qPCR

RNA of iPSCs and iPS-cell derived CD34+ HSPCS and CD61+ MKs was isolated using the RNeasy Mini Kit (QIGAEN GmbH, Hilden, Germany) according to manufacturer's protocol. RNA (500 ng) was used for cDNA synthesis. Quantitative RT-qPCR was performed using the 7500 Fast Real-time PCR System (Applied Biosystems by Life technologies, Paisley, UK) with the SYBR Select Master Mix for CFX (Applied Biosystems). The sequences of primers used for-qPCR are listed in Table S7. All primers were purchased from Eurofins-MWG biotech (Ebersberg, Germany). The mRNA expression level of the target gene is determined in % of *GAPDH* or *MT-ATP6*.

SDS-page and Western blot

SDS-Page and Western blot analysis were conducted as previously described (Han et al., 2016). Primary and secondary antibodies are listed in Table S6.

Undirected hematopoietic differentiation of iPSCs into hematopoietic progenitors and myeloid subsets with the "EB-based" protocol

iPSCs were cultured on irradiated mouse embryonic fibroblast feeder layer in KnockOut-DMEM based iPSC medium. More detailed information regarding cell culture conditions can be found in Table S8.

For the generation of iPSC-derived CD34+ HSPCs, CALR iPSCs were subjected to mesoderm commitment and hematopoietic differentiation with an embryonic body (EB)-based protocol modified from the differentiation method described by Kovarova and colleagues (Kovarova and Koller, 2012). CD34+ HSPCs were cultured and differentiated into myeloid subsets in the StemPro 34 SFM medium (Thermo Fisher Scientific) based progenitor medium at the maximum density of $1x10^6$ cells/ml. Details of EB and HSPCs differentiation media are provided in Table S8.

Differentiation of iPSCs into hematopoietic stem cells and myeloid subsets with the "spin-EB" protocol

Feeder-free iPSC culture was maintained on matrigel coated 6-well plates and routinely passaged with 1 ml accutase or 0.5 mM EDTA (Thermo Fisher Scientific). To enhance single cell survival, 10 µM ROCK inhibitor Y-27632 was added to the maintenance culture medium StemMACs iPS Brew XF for 24 h after seeding. iPSC medium was changed daily.

Human iPSCs were differentiated into HSPCs, MKs and erythrocytic cells adapted from the differentiation protocol by Liu et. al (Liu et al., 2015). Briefly, iPSCs were seeded into U-bottom-shaped 96-well plates with a density of 3,000 cells/well in cytokine supplemented serum-free medium (SFM). To allow spheroid formation, plates were spun at 380 g for 5 min. From day 2 to day 8, cells were cultured in SFM with 10 ng/ml VEGF (Miltenyi Biotec), 10 ng/ml BMP4 (Miltenyi Biotec), 10 ng/ml bFGF (Peprotech, Hamburg, Germany) and SCF (0.5 % supernatant of SCF secreting CHO KLS cells). From day 8 onwards, BMP4 and VEGF were removed from the medium. On day 11, 20 ng/ml TPO (Miltenyi Biotec) was added to the medium. On day 14, cells were harvested and filtered through a 100 µm filter to separate the EBs from the suspension cells. Single cells were analyzed by flow cytometry and purified for CD61+ and CD34+ cell fractions. More detailed information on SFM Medium is given in Table S8.

Cell morphology analysis

Phase contrast images of iPSC generation and differentiation were obtained with EVOS FL microscope (Thermo Fisher Scientific). To characterize the morphologies of iPSC-derived precursors and myeloid subsets, cells were spun onto slides with Shandon Cytospin 4

cytocentrifuge (Thermo Fisher Scientific) and stained with Diff Quik solution 1 and 2 (Medion Diagnostics, Düdingen, Switzerland) after methanol fixation. Images were acquired using a Leica DMRX microscope and Leica Application Suite software (Leica Microsystems).

MPO cytochemical staining

In order to evaluate MPO functional activity, iPSC-derived hematopoietic cells at differentiation day 15 were centrifuged onto slides and fixed with LEUCOGNOST® Fixing Mixture. The fixed cells were stained with LEUCOGNOST® POX Kit according to the manufacturer's instructions. Counterstaining of nucleus was performed using Mayer's hemalum solution and slides were mounted with Kaiser's glycerol gelatin (the Kit and all reagents were obtained from Merck Millipore). Images were acquired as described above.

Flow cytometry analysis

To evaluate cell surface progenitor and lineage specific markers, single cells were analyzed on day 10, day 12 and day 14 of "spin-EB" differentiation and on day 10 and day 15 of "EB-based" differentiation. Cells were harvested and passed through a 100 µm cell strainer, centrifuged at 350 g for 5 min. After washing with ice cold FACS buffer, single cells were incubated with lineage-specific antibodies at 4°C for 30 min. Stained cells were resuspended in 300 µl FACS buffer and analyzed on a FACS Canto II (BD). All staining and washing steps were performed in FACS buffer consistent of PBS supplemented with 2 mM EDTA and 2 % BSA (PAN Biotech, Aidenbach, Germany).

To identify the intracellular MPO expression, differentiated hematopoietic cells at day 15 of "EB-based" differentiation were fixed and permeabilized using Fix & Perm Cell Permeabilization Kit (Thermo Fisher Scientific). Cells were firstly stained for cell surface markers CD15 and CD45 for 20 min at room temperature (RT), followed by intracellular MPO staining for 20 min at RT after fixation and permeabilization. Stained cells were evaluated by Gallios flow cytometer (Beckman Coulter, Krefeld, Germany). All data were analyzed by FlowJo™ (version 10, Oregon, USA).

Full list of antibodies is summarized in Table S5. In each experiment matched Ig isotype controls were used to set background fluorescence.

CRISPR/Cas9-mediated repair of homozygous *CALRins5* and *CALRdel52* mutation in iPSCs

The Alt-R™ CRISPR-Cas system (Integrated DNA Technologies IDT, Coralville, USA) was used to efficiently correct homozygous *CALRins5* or *CALRdel52* mutations in MPN patient-specific iPSCs. For precise editing the Alt-R® S.p HiFi Cas9 Nuclease V3 was used together with a single-stranded donor template to repair the double strand break by the cellular

repair mechanisms of homology directed repair (HDR). In brief, guide RNA composing of crRNA and tracrRNA was combined with HiFi. Cas9 Nuclease to assembly the CRISPR-Cas9 ribonucleoprotein complex. Singularized iPSCs were gently mixed with the ribonucleoprotein complex, single-stranded donor template, and electroporation enhancer. Nucleofection was performed using the 4D NucleofectorTM X-Unit and the P3 Primary Cell 4D-NucleofectorTM X, Kit S (both from Lonza, Basel, Switzerland). HDR was stimulated by HDR enhancer (IDT, Coralville, USA). After nucleofection, iPSCs were seeded on previously coated Laminin 521 (Biolamina, Sundbyberg, Sweden) plates to support cell viability in StemMACS™ iPS-Brew XF (Miltenyi Biotec, Bergisch Gladbach, Germany) supplemented with 10 µM of Rock inhibitor Y-27632 and 1x CloneR (Stemcell Technologies). Repair of *CALR*ins5 and *CALR*del52 mutation was verified by allele-specific or flanking PCR, respectively, and proofed by Sanger sequencing and Western blot. Possible off-target effects were excluded by PCR reaction of off-target sites and subsequent Sanger sequencing. Sequences of crRNA, donor template and primers are provided in Table S2 and 3.

Purification of CD34+ HSPCs and CD61+ megakaryocytes by magnetic activated cell sorting

On day 25-35 of "EB-based" differentiation and on day 14 of "spin-EB" differentiation anti-CD34 and anti-CD61 MicroBeads (Miltenyi Biotec, Bergisch Gladbach, Germany) were used to separate HSPCs and MKS, respectively. Purification of cells was performed according to the protocol provided by the manufacturer. In brief, single cell suspension was incubated with CD61 or CD34 MicroBeads for 15 or 30 min, respectively, to label the cells magnetically. Cell suspension was loaded onto a LS column installed in a magnetic field. After washing three times with MACS buffer consisting of PBS supplemented with 5 % FCS (Thermo Fisher Scientic) and 2 mM EDTA to remove unbounded cells, the column was removed from the magnetic field and positively selected cell fraction was eluted with 5 ml of MACS buffer from the column. After centrifugation at 300 g for 10 min, purified cells were counted and further processed. CD61+ MKs and CD34+ HSPCs were either snap frozen for RT-qPCR or used for transmission electron microscopcy or seeded in Colony-Forming Unit Assay, respectively.

Colony-forming unit assay of CD34+ HSPCs

Purified CD34+ cells were seeded in MethoCult^{TM} (Stemcell Technologies) supplemented with 20 ml IMDM (Thermo Fisher Scientific), 50 ng/ml hSCF, 10 ng/ml hIL-3. 10 ng/ml hGMSCF and 14 ng/ml hEPO (all ImmunoTools Friesoythe; Germany) in a cell density of 5,000 cells/ml. After 10-12 days of culture at 37° C, colonies were identified and counted based on morphology using light microscopy (Motic, Barcelona, Spain).

Transmission electron microscopy

iPSC-derives CD61+ megakaryocytes at day 14 of “spin-EB” differentiation were prepared as described previously. Purified MKs were washed with PBS and fixed with 3 % glutaraldehyde for at least 2 h at RT, followed by embedding in 5 % low melting agarose (Merck). Gelatinated blocks were washed in 0.1 M Soerensen’s phosphate buffer (Merck) and post-fixed in 17 % sucrose buffer (Merck) containing 1 % OsO4 (Roth, Karlsruhe, Germany). Subsequently, specimens were dehydrated performing an ascending ethanol series repeating the last step for three times (30, 50, 70, 90, and 100 % ethanol; 10 min each step). Dehydrated samples were consecutively incubated in propylene oxide (Serva, Heidelberg Germany) for 30 min, in a mixture of EPON resin (Serva) and propylene oxide (1:1) for 1 h, and in pure EPON for 1 h. EPON polymerization was conducted at 90 °C for 2 h. Ultrathin sections of 70−100 nm were cut with a Reichert Ultracut S ultramicrotome (Leica, Wetzlar, Germany) equipped with a diamond knife (Leica) and picked up on copper−rhodium grids (Plano, Wetzlar, Germany). Contrast was enhanced by staining with 0.5 % uranyl acetate and 1 % lead citrate (both EMS, Munich, Germany). Samples were viewed at an acceleration voltage of 60 kV using a Zeiss Leo 906 (Carl Zeiss, Jena, Germany) transmission electron microscope. Image processing and analysis was performed using ImageJ (Schneider et al., 2012).

Preparation of samples for RNA Sequencing

RNA of purified CD61+ MKs was isolated as described in Supplementary Information. Quality was verified by TapeStation 4200 (Agilent, Santa Clara, USA) to determine RNA integrity number (RIN). RNA concentration was measured with Fluorometer Quantus™ (Promega, Fitchburg, USA). According to manufacturer’s protocol, ribosomal RNA was depleted using NeBNext® rRNA Depletion Kit, prior to library preparation with NeBNext®Ultra™II Directional RNA Library Prep Kit for Illumina (both New England BioLabs, Ipswich, USA) using an RNA input of 100 ng per sample (New England BioLabs, Ipswich, USA). Subsequently, samples were sequenced in paired end reads (2x76 bp, dual indexed) on two NextSeq High Output Kits v2.5 (150 cycles) on a NextSeq 500 instrument (both Illumina, San Diego, USA) to have sufficient reads for data analysis.

4. References

Han, L., Schubert, C., Köhler, J., Schemionek, M., Isfort, S., Brümmendorf, T.H., Koschmieder, S., and Chatain, N. (2016). Calreticulin-mutant proteins induce megakaryocytic signaling to transform hematopoietic cells and undergo accelerated degradation and Golgi-mediated secretion. J. Hematol. Oncol. *9*, 1–14.

Kirschner, M., Maurer, A., Wlodarski, M.W., Ventura Ferreira, M.S., Bouillon, A.-S., Halfmeyer, I., Blau, W., Kreuter, M., Rosewich, M., Corbacioglu, S., et al. (2018). Recurrent somatic mutations are rare in patients with cryptic dyskeratosis congenita. Leukemia *32*, 1762–1767.

Kovarova, M., and Koller, B. (2012). Differentiation of mast cells from embryonic stem cells. Curr. Protoc. Immunol.

Liu, Y., Wang, Y., Gao, Y., Forbes, J.A., Qayyum, R., Becker, L., Cheng, L., and Wang, Z.Z. (2015). Efficient Generation of Megakaryocytes From Human Induced Pluripotent Stem Cells Using Food and Drug Administration-Approved Pharmacological Reagents. Stem Cells Transl. Med. *4*, 309–319.

Schneider, C.A., Rasband, W.S., and Eliceiri, K.W. (2012). NIH Image to ImageJ: 25 years of image analysis. Nat. Methods *9*, 671–675.

Szabo, E., Rampalli, S., Risueño, R.M., Schnerch, A., Mitchell, R., Fiebig-Comyn, A., Levadoux-Martin, M., and Bhatia, M. (2010). Direct conversion of human fibroblasts to multilineage blood progenitors. Nature *468*, 521–526.

Theocharides, A.P.A., Lundberg, P., Lakkaraju, A.K.K., Lysenko, V., Myburgh, R., Aguzzi, A., Skoda, R.C., and Manz, M.G. (2016). Homozygous calreticulin mutations in patients with myelofibrosis lead to acquired myeloperoxidase deficiency. Blood *127*, 3253–3259.